SEMARAK ILMU PUBLISHING

Journal of Advanced Research in Fluid Mechanics and Thermal Sciences

Journal homepage:
https://semarakilmu.com.my/journals/index.php/fluid_mechanics_thermal_sciences/index
ISSN: 2289-7879

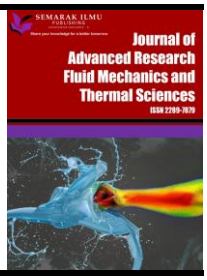

Study Optimal Approximation Solution of First Grade Fluid Flow with Slip Boundary Condition by Optimal Perturbation Iteration Algorithm

Batool Abdulhakeem Badea[1,*], Abeer Majeed Jasim[1]

[1] Department of Mathematics, College of Science, University of Basrah, Basrah, Iraq

ARTICLE INFO

Article history:
Received 30 October 2024
Received in revised form 27 February 2025
Accepted 8 March 2025
Available online 20 March 2025

Keywords:
Optimal perturbation iteration algorithm; convergence analysis; squeezing flows; magnetohydrodynamics; slip boundary condition

ABSTRACT

In this article, the steady two-dimensional axis metric flow of an incompressible viscous fluid in a porous medium under the influence of a uniform transverse magnetic field with slip boundary condition is analyzed and solved by using perturbation iteration algorithm (PIA) and optimal perturbation Iteration Algorithm. The optimal perturbation iteration algorithm (OPIA) has been used to obtain the approximate analytical solution by varying the pertinent flow parameters. The influence of different parameters on the present flow solution is shown through graphs with a discussion. These graphs refer to the fact that increasing numbers of Reynolds and Hartmann give the attribute of decreasing velocity, with the addition that with an increase in Hartmann number and decrease in Reynolds number the streamlines are stretched towards the x-axis. Finally, the optimal perturbation iteration algorithm is effective and highly able to obtain excellent results.

1. Introduction

Squeezing flows occur when normal stresses or vertical velocities are applied from the outside by the mobile boundary [1]. Squeezing flow under the influence of a magnetic field has many applications in chemical engineering, as studied by many researchers. Precise applications have begun to study groundwater flow, Irrigation problems, crude petroleum recovery, heat-storage beds, thermal and insulating engineering, chromatography, and chemical catalytic reactors. The study of thin Newtonian liquid films squeezed between plates is investigated by Grimm [2]. For the first time Navier has been the general boundary conditions, which shows the fluid slip at the surface [3]. Near the boundary, a molecule shows slips at the boundary when the molecular weight is high. According to Navier, the difference between fluid velocities and the boundary is proportional to shear stress at that boundary. The constant of proportionality is called the slip parameter. The slip condition is significant when a fluid with elastic character is considered. In medical sciences, particularly in polishing artificial heart valves and internal cavities, the slip condition is highly considered [4,5]. The most practical examples of squeezing flows are polymer processing, compression, and injection

* *Corresponding author.*
E-mail address: batoolabdulhakeem@gmail.com

https://doi.org/10.37934/arfmts.128.2.226246

modeling. The Newtonian squeezing fluid flow between two parallel plates is studied by Ran *et al.,* [6]. The effects of slip boundary conditions are investigated by Hayat and Abelman [7] Newtonian fluid was considered by Ebaid [8] to study the effects of a magnetic field and wall slip boundary conditions on the peristaltic transport in an asymmetric channel. The same model with the extension of the porous medium is argued by Abelman *et al.,* [9]. Ullah *et al.,* [10] studied squeezing fluid flow between the two infinite parallel plates in a porous medium channel. Hayat *et al.,* [11] examined the hydromagnetic three-dimensional flow induced by a stretched surface and thermal slip boundary conditions. Shafiq *et al.,* [12] have investigated the squeezed flow of a third-grade fluid between two parallel disks and heat transfer in the flow is characterized by the Cattaneo-Christov theory electrically conductive flow through the porous mentioned has gained exceptional rank and was the point of interest of many scientific studies. There are many applications of magnetohydrodynamics (MHD) of an electrically conducting fluid in geophysics astrophysics, engineering, and other industrial areas. More to the point, the flows of electrically conducting fluid problems through porous medium have acquired exceptional rank and have been the spotlight of interest of many researchers [13-18]. And others have studied this method [19-23]. However, there is a limited number of these problems, and most of them do not have an exact solution. Therefore, several semi-analytical methods are used to solve the governing equations of fluid flow problems. Among the widely used analytical methods are turbulence methods that were used to determine the effect of physical parameters on the velocity profile, and One method was used in this research, namely using perturbation Iteration Algorithm. The current study aims to find the optimal approximate analytical solution through an optimal perturbation Iteration Algorithm and test the accuracy of the solution by studying the effect of physical parameters on the velocity profile, testing the convergence of these solutions, and comparing the outcome and the numerical solution obtained by BVP4C with other methods. The organization of this paper is as follows: The governing equations are derived in section 3. Details of the derivation of the perturbation Iteration Algorithm and optimal perturbation Iteration Algorithm have been written as steps in section 2. The performance of the perturbation Iteration Algorithm for first-grade MHD squeezing fluid flow with OPIA is applied in section 4. In section 5 the convergence analysis is presented. Results and discussions are given in section 6.

2. Perturbation Iteration Algorithm

Perturbation is an important class of iterative methods of analytical techniques, that are used to find approximate solutions of differential equations, integral-differential equations, and nonlinear algebraic equations [1]. These techniques are useful in clarifying, predicting, and characterizing phenomena caused by nonlinear processes in vibratory systems. Mathematical techniques for estimating differential equations are referred to as approximate solution by starting with the exact solution of the simpler equations which can be defined as perturbation methods. When a problem lacks a known precise solution but can be described as a minor modification to a known solvable problem, perturbation is frequently utilized. Perturbation iteration is used in a wide range of Physical fields. To explain the idea of the standard perturbation iteration algorithm PIA (1,1), consider the nonlinear ordinary differential equation as a form [29];

$$D\left(z, A(z), \frac{dA}{dz}, \frac{d^2A}{dz^2}, \frac{d^3A}{dz^3}, \dots, \frac{d^{n-1}A}{dz^{n-1}}, \frac{d^nA}{dz^n}\right) = 0, \tag{1}$$

where D is a function of A and its derivatives**,** A is an unknown function and denotes z spatial dependent variable. In Eq. (1), the auxiliary perturbation parameter can be add as shown in the following equation:

$$D\left(z, A(z), \frac{dA}{dz}, \frac{d^2A}{dz^2}, \frac{d^3A}{dz^3}, \dots, \frac{d^{n-1}A}{dz^{n-1}}, \frac{d^nA}{dz^n}, \varepsilon\right) = 0\,, \tag{2}$$

Now, rearranging the writing of Eq. (1) as follows:

$$D\left(z, A_{m+1}(z), \frac{dA_{m+1}}{dz}, \frac{d^2A_{m+1}}{dz^2}, \frac{d^3A_{m+!}}{dz^3}, \dots, \frac{d^{(n-1)}A_{m+1}}{dz^{n-1}}, \frac{d^nA_{m+1}}{dz^n}, \varepsilon\right) = 0\,, \tag{3}$$

m represents the mth iteration with defined perturbation expansions with correction term for $m = 0,1,2, \dots$ as follows:

$$\begin{aligned} A_1 &= A_0 + \varepsilon(A_c)_0\,, \\ A_2 &= A_1 + \varepsilon(A_c)_1\,, \\ A_3 &= A_2 + \varepsilon(A_c)_2\,, \\ &\vdots \\ A_{m+1} &= A_m + \varepsilon(\mathrm{A}_c)_{\,m}\,, \end{aligned} \tag{4}$$

where ε is a small perturbation parameter and A_c is the correction term in the perturbation expansion. Furthermore, substituting Eq. (4) in Eq. (3), give

$$D(z, A_m(z) + \varepsilon(A_c)_n, A'_m(z) + \varepsilon(\mathrm{Ac})'_m, A''_m(z) + \varepsilon(\mathrm{Ac})''_m, A'''_m(z) + \varepsilon(\mathrm{Ac})'''_m, \dots, \quad A_m^{n-1}(z) + \varepsilon\left(A_c^{(n-1)}\right)_m, A^n(z) + \varepsilon\left(A_c^{(n)}\right)_m, \varepsilon) = 0, \tag{5}$$

in the next step, we take the Taylor series expansion for the first order derivative in the neighbourhood of $\varepsilon = 0$, yields

$$D\left(z, A_{m+1}(z), \frac{dA_{m+1}}{dz}, \frac{d^2A_m}{dz^2}, \frac{d^3A_{m+1}}{dz^3}, \dots, \frac{d^{(n-1)}A_{m+1}}{dz^{(n-1)}}, \frac{d^nA_{m+1}}{dz^n}, \varepsilon\right) +$$

$$\varepsilon\frac{dD}{dA_m}.(A_c)_m + \varepsilon\frac{dD}{dA'_m}(A_c)'_m + \varepsilon\frac{dD}{dA''_m}.(A_c)''_m + \cdots + \varepsilon\frac{dD}{dA^{n-1}}.(A_c)^{n-1}{}_m$$

$$+\varepsilon\frac{dD}{dA^n}.(A_c)^n_m + \varepsilon = 0, \tag{6}$$

$$(A_c)_m^{(n)} = \frac{D}{\varepsilon.\frac{dD}{dA_m^{(n)}}} - \frac{\frac{dD}{dA_m}}{\frac{dD}{dA_m^{(n)}}}.(A_c)_m - \frac{\frac{dD}{dA'_m}}{\frac{dD}{dA_m^{(n)}}}.(A_c)'_m - \cdots - \frac{\frac{dD}{dA_m^{(n-1)}}}{\frac{dD}{dA_m^{(n)}}}.(A_c)_m^{(n-1)} - \frac{\frac{dD}{d\varepsilon}}{\frac{dD}{dA_m^{(n)}}}. \tag{7}$$

Now, all calculations in Eq. (7) are performed at $\varepsilon = 0$ and result in the ordinary differential equation. This ordinary differential equation is solved to obtain $(A_c)_m(z)$. To find the first correction term, substitute A_0 into Eq. (7). Where A_0 is a trial function satisfying the initial condition. The first correction can be introduced as follows:

$$(A_c)_0^{(n)} = \frac{-D}{\varepsilon\frac{dD}{dA_0^{(n)}}} - \frac{\frac{dD}{dA_0}}{\frac{dD}{dA_0^{(n)}}}.(A_c)_0 - \frac{\frac{dD}{dA'_0}}{\frac{dD}{dA'^{(n)}_0}}.(A_c)'_0 - \cdots - \frac{\frac{dD}{dA_0^{n-1}}}{\frac{dD}{dA_0^{(n)}}}.(A_c)_m^{n-1} - \frac{\frac{dD}{d\varepsilon}}{\frac{dD}{dA_0^n}} \tag{8}$$

To obtain a more effective and better approximation, it can give a basic idea about the optimal iterative perturbation method [25]. The proposed approach to perturbation is iterative based on the idea of the Homotopy analysis method. The new construction includes convergence parameters that are symbolized by $\beta_0, \beta_1, \beta_2, \ldots$. These parameters can be entered into Eq. (4) to obtain new components. These components have been described by

$$\begin{aligned} &A_1(z,\beta_0) = A_0 + \beta_0 (A_c)_0\,, \\ &A_2(z,\beta_1) = A_1 + \beta_1 (A_c)_1\,, \\ &A_3(z,\beta_2) = A_2 + \beta_2 (A_c)_2\,, \\ &\vdots \\ &A_m(\mathrm{z},\beta_{m-1}) = A_{m-1} + \beta_{m-1} (\mathrm{A}_c)_{\,m-1}\,, \end{aligned} \tag{9}$$

To obtain optimal values of these parameters, replace the approximate analytical solution in Eq. (1). The residual functional can be defined by formulation as follow:

$$\tilde{R}(z,\beta_0,\beta_1,\beta_2,\ldots,\beta_{m-1}) = D\left(A_m^{(n)}, A_m^{(n-1)}, \ldots, A_m'''', A_m''', A_m'', A_m\right), \tag{10}$$

To obtain the optimum values of theses parameters, substituting the approximate analytical solution in Eq. (1) The case can be clarified, when $\tilde{R}(z,\beta_0,\beta_1,\beta_2,\ldots,\beta_{m+1}) = 0$, then the approximation A_m is the exact solution of the problems. Normally, such a situation does not occur in nonlinear equations, but one can minimize the functional

$$\tilde{J}(\beta_0,\beta_1,\beta_2,\ldots,\beta_{m-1}) = \int_a^b \tilde{R}^2(z,\beta_0,\beta_1,\beta_2,\ldots,\beta_{m-1})dz, \tag{11}$$

where a and b are selected from the domain of the problem. The optimum values of $\beta_0, \beta_1, \beta_2, \ldots$ can be optimally defined based from the conditions

$$\frac{d\tilde{J}}{d\beta_0} = \frac{d\tilde{J}}{d\beta_1} = \cdots = \frac{d\tilde{J}}{d\beta_{m-1}} = 0. \tag{12}$$

3. The Formulation of the Problem

Here, the squeezing flow of an incompressible Newtonian fluid under consideration with constant density ρ and viscosity μ between two large planar parallel plates approaching each other at a low constant velocity $\breve{U}$ in the presence of a magnetic field. The plates are separated by a small distance of $2L$ can be seen in Figure 1. The flow is assumed to be quasi-steady [3,10]. The flow is controlled by the Navier-Stokes equations when inertial terms are retained. These equations, which can be derived from the conservation equations, which represent the continuity equations and the momentum equation, can be presented in the Cartesian form as follows:

$$\nabla.\breve{U} = 0, \tag{13}$$

$$\rho\left[\frac{\partial \breve{U}}{\partial} + \left(\nabla.\breve{U}\right).\breve{U}\right] = \nabla.\boldsymbol{w} + \left(\breve{U} \times \boldsymbol{H}\right) \times \boldsymbol{H}, \tag{14}$$

where, ∇ denotes the derivative of material time and $\boldsymbol{w}$ is the Cauchy stress tensor can be defined by

$$\boldsymbol{w} = -pI + \mu(\nabla u + (\nabla u)^T), \tag{15}$$

$\boldsymbol{H}$ is the total magnetic field given by $\boldsymbol{H} = \boldsymbol{H_0} + b$. b and $\boldsymbol{H_0}$ are the induced and imposed magnetic fields, respectively. The Maxwell equation and modified Ohm's law in the absence of displacement currents, are

$$N = \delta\left[E + \breve{\boldsymbol{U}} \times \boldsymbol{H}\right], \qquad \nabla \cdot \boldsymbol{H} = 0, \tag{16}$$

$$\nabla \times \boldsymbol{H} = \mu_p N, \qquad curl\ E = \frac{\partial \boldsymbol{H}}{\partial t}. \tag{17}$$

In this case, N is the density of electric current, δ represents electrical conductivity, E is the electric field, and μ_p is the magnetic permeability.

If ρ, and δ are constant, the force of MHD can be expressed as follows:

i. b is insignificant in relation to B_0.
ii. B is perpendicular to $\breve{U}$ such that the Reynold number is minimal.
iii. There is no electric field in the fluid flow zone.

which of the above points fulfills the following equation?

$$N \times \boldsymbol{H} = -\delta \boldsymbol{H_0^2} \breve{U}, \tag{18}$$

The plates are non-conductive, and the magnetic field is applied along the z-axis. The gap distance $2L$ between the two plates changes slowly with time t for small values of velocity so that it can be considered constant. An axisymmetric flow in cylindrical coordinates (r, θ, z) with $\breve{U}$ the axis perpendicular to plates and $z = \pm L$ at the plates. Furthermore, axial symmetry, $\breve{U}$ is represented by $\breve{U} = \left(\breve{U}_r, 0, \breve{U}_z\right)$. Due to the negligible body forces with no tangential velocity, the Navier-Stokes equation in the cylindrical coordinates can be presented in the form of a mathematical model as follows [1,10,24]:

$$\frac{\partial \mathrm{p}}{\partial r} - \rho\Lambda\, \breve{U}_z = -\mu \frac{\partial \Lambda}{\partial z} - \delta H_0^2 \breve{U}_r, \tag{19}$$

$$\frac{\partial \mathrm{p}}{\partial z} + \rho\Lambda \breve{U}_r = \frac{\mu}{r}\, \frac{\partial}{\partial r}\, (r\Lambda), \tag{20}$$

where,

$$\Lambda(r, z) = \frac{\partial\, \breve{U}_z}{\partial r} - \frac{\partial \breve{U}_r}{\partial z} \tag{21}$$

the definition of the stream function $\xi(r, z)$ canbe introduce by

$$\breve{U}_r = \frac{1}{r}\, \frac{\partial \xi}{\partial r}, \breve{U}_z = -\frac{1}{r}\, \frac{\partial \xi}{\partial r}, \tag{22}$$

The pressure can be eliminated by deriving Eq. (19) with respect to z and Eq. (20) with respect to r and then subtracting the two resulting equations, become

$$\rho\left[\frac{\partial\left(\xi, E^2, \frac{\xi}{r^2}\right)}{\partial(r,z)}\right] = -\frac{\mu}{r}N^4\xi + \delta\frac{\boldsymbol{H_0^2}}{r}\frac{\partial^2}{\partial z^2}, \tag{23}$$

where

$$N^2 = \frac{\partial^2}{\partial r^2} - \frac{1}{r}\frac{\partial}{\partial r} + \frac{\partial^2}{\partial z^2}, \tag{24}$$

Using the appropriate transformation it can be written in the following form

$$\xi(r,z) = r^2\, a(z), \tag{25}$$

Using the appropriate transformation it can be written in the following form

$$\xi(r,z) = r^2\, a(z)\,, \tag{25}$$

by substituting an Eq. (25) into Eq. (23), the following arrangement is the result

$$a''''(z) - \frac{\delta H_0^2}{\mu}\, a''(z) + 2\frac{\rho}{\mu}\, a(z)a'''(z) = 0, \tag{26}$$

The initial and slip boundary conditions are

$$a(0) = 0, \quad a''(0) = 0, \quad a(L) = \frac{\gamma}{2}, \quad a'(L) = \pi a''(L), \tag{27}$$

Non-dimensional parameters can be described as:

$$A^* = \frac{\frac{a}{\gamma}}{2}, \; z^* = \frac{z}{L}, \quad Re = \frac{\frac{\rho L}{\mu}}{\gamma}, M = \frac{H_0 L\sqrt{\delta}}{\mu}. \tag{28}$$

After putting Eq. (28) into Eq. (26) and Eq. (27) and removing $*$, becomes

$$\frac{d^4A(z)}{dz^4} - M^2\frac{d^2A(z)}{dz^2} + ReA(z)\frac{d^3A(z)}{dz^3} = 0, \tag{29}$$

$$A(0) = 0\,, \; \frac{d^2A(0)}{dz^2} = 0, \; A(1) = 1, \; \frac{dA(1)}{dz} = Y\frac{d^2A(1)}{dz^2}, \tag{30}$$

The symbols of non-dimensional are $Y = \frac{\pi}{L}$ representing the slip parameter, Re is the Reynolds number and M is the Hartmann number.

i. **Reynolds Number:** is a dimensionless number used in fluid mechanics to describe the flow behavior .it determines whether the flow is laminar or turbulent.
ii. **Hartmann Number:** is a dimensionless number used in Magnetohydrodynamics (MHD)to measure the effect of a magnetic field on the behavior of conducting fluid. **Summary**
iii. **Reynolds Number** is used to determine the type of flow.
iv. **Hartmann Number** is used to measure the effect of the magnetic field on conduction fluids.

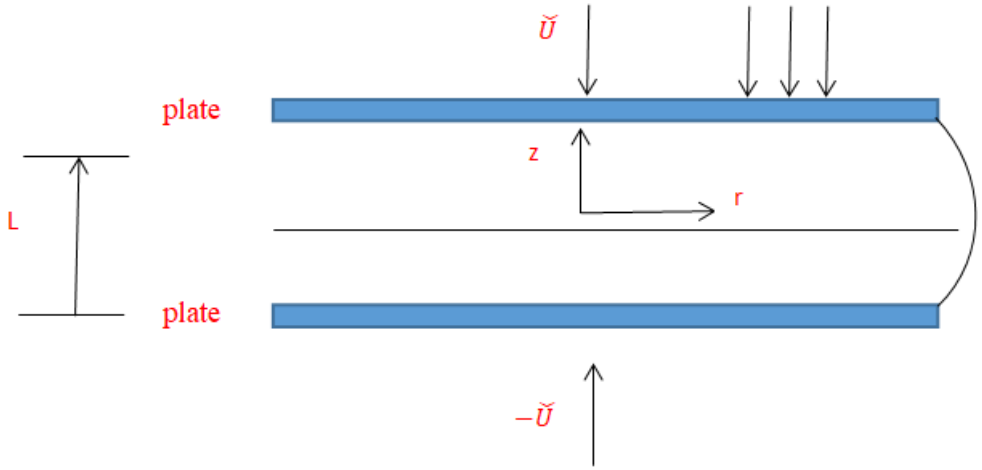

Fig. 1. A steady squeezing axisymmetric fluid flow between two parallel plates

4. The Application of PIM and OPIM for the Problem

The PIA and OPIM apply several steps to the nonlinear differential Eq. (29) to find an analytical approximation solution. The problem of the auxiliary perturbation parameter ε are

$$D\left(A(z),\frac{d^2A}{dz^2},\frac{d^3A}{dz^3},\frac{d^4A}{dz^4},\varepsilon\right)=\frac{d^4A}{dz^4}-M^2\varepsilon\frac{d^2A}{dz^2}+Re\varepsilon A(z)\frac{d^3A}{dz^3}, \tag{31}$$

perturbation expansions with only one correction term are given as follows:

$$A_{m+1}=A_m+\varepsilon(A_c)_m, \tag{32}$$

substituting Eq. (32) into Eq. (31), the Taylor series with first-order derivative terms about $\varepsilon=0$, yields

$$D(A_m,A_m'',A_m''',A''''_m0)+\varepsilon[D_{A_m}(A_c)_m+D_{A''_m}(A_c)''_m+D_{A'''_m}(A_c)'''_m+D_{A''''_m}(A_c)''''_m+D_\varepsilon]=0, \tag{33}$$

the following derivatives

$$\begin{aligned}
&D_{A_m}=Re\varepsilon\frac{d^3A_m(z)}{dz^3},\\
&D_{A''_m}=-M^2\varepsilon,\\
&D_{A'''_m}=Re\varepsilon A_m(z),\\
&D_{A''''_m}=1,\\
&D_\varepsilon=-M^2\frac{d^2A}{dz^2}++ReA_m(z)\frac{d^3A_m(z)}{dz^3},\\
&D(A_m(z),A_m''(z),A_m'''(z),A_m''''(z),0)=\frac{d^4A_m(z)}{dz^4},
\end{aligned} \tag{34}$$

calculating all derivatives at $\varepsilon=0$ and substituting the results into (33) yields the following linear ordinary differential equations:

$$(A_c)''''_m=\frac{-1}{\varepsilon}A''''_m(z)+M^2A_m''(z)-ReA_m(z)A_m'''(z), \tag{35}$$

assume that the initial condition,

$$A_0(z) = \alpha_0 + \alpha_1 z + \frac{\alpha_2}{2} z^2 + \frac{\alpha_3}{3!} z^3, \tag{36}$$

where,

$$A(0) = \alpha_0 \ , \quad \frac{dA(0)}{dz} = \alpha_1 \ , \quad \frac{d^2A(0)}{dz^2} = \alpha_2 \ , \quad \frac{d^3A(0)}{dz^3} = \alpha_3,$$

from the boundary condition (30), become

$$A_0(z) = \alpha_1 z + \frac{\alpha_3}{6} z^3, \tag{37}$$

Nevertheless, there are two cases for the solving of Eq. (29). Firstly, the solution results from PIM that contains α_2 and α_3 is unknown. These values can be extracted with the help of boundary conditions. The approximate analytical solutions to Eq. (29) resulting from PIM are as follows:

$$A_1 = \alpha_1 z + \frac{1}{6}\alpha_3 z^3 - 0.20000000000(0.04166666667 Re\alpha_2\alpha_3 - 0.04166666667 M^2\alpha_3)z^5 - 0.0001984126984 Re\alpha_3^2 z^7 \ , \tag{38}$$

$$A_2 = \alpha_1 z + \frac{1}{6}\alpha_3 z^3 + (-0.0833333333 Re\alpha_2\alpha_3 + 0.083333333 M^2\alpha_3)z^5 + (0.00198412698 Re \alpha_3^2 + 0.001190476191 M^2(-0.16666666666 Re\alpha_2\alpha_3 + 0.166666666 M^2\alpha_3) - 0.00119047619 Re\alpha_1(-0.5000000000 Re\alpha_2\alpha_3 + 0.5000000000 M^2\alpha_3))z^7 + (-0.000002755731924 M^2 Re\alpha_3^2 + 0.0000137785962 Re^2\alpha_1\alpha_3^2 - 0.0000551463848 Re\alpha_3(-0.50000000000 Re\alpha_2\alpha_3 + 0.5000000 M^2\alpha_3) - 0.0003306848 Re(-0.0083333333334 Re\alpha_2\alpha_3 + 0.008333333334 M^2\alpha_3)\alpha_3)z^9 + (9.0187508181\ 10^{-7} Re^2\alpha_3^2 - 0.000126262626 Re(-0.0083333333334 Re\alpha_2\alpha_3 + 0.003333333 M^2\alpha_3)(0.50000000 Re\alpha_2\alpha_3 + 0.50000000 M^2\alpha_3))z^{11} + (0.00002428127428 Re^2(-0.008333333 Re\alpha_2\alpha_3 + 0.00833333334 M^2\alpha_3)\alpha_3^2 + 1.1562511556\ 10^{-8} Re^2\alpha_3^2(-0.5000000000 Re\alpha_2\alpha_3 + 0.500000000 M^2\alpha_3))z^{13} - 2.523564031\ 10^{-10} Re^3\alpha_3^4 z^{14} \ , \tag{39}$$
⋮

Second, the solution result from OPIM that contains $\alpha_1, \alpha_3, \beta_0$ and β_1 are unknown. The values of α_1 and α_3 can be extracted with the help of boundary conditions and the values of β_0 and β_1 can be extracted by finding the residual and then applying the basic condition for minimize functional. The approximate analytical solutions to Eq. (29) resulting from OPIM are as follow:

$$A_1 = \alpha_1 z + \frac{1}{6}\alpha_3 z^3 - (0.200000000(0.04166666667\alpha_1\alpha_3 - 0.0416666667\ \alpha_3 z^5 + \beta_0(-0.000198412684\alpha_3^2)z^7 \ , \tag{40}$$

$$A_2 = \alpha_1 z + \frac{1}{6}\alpha_3 z^3 + ((-0.00833333330\beta_0(-1. Re\alpha_2\alpha_3 + M^2\alpha_3) + 0.008333333330 M^2\alpha_3 - 0.008333333330 Re\alpha_2\alpha_3)\beta_1 + (0.00833333333 Re\ \alpha_2\alpha_3 \quad +0.00833333333 M^2\alpha_3))z^5 + +((0.000198412698309 Re\beta_0\alpha_3^2 + 0.001190476191 M^2\beta_0(-0.16666666667 Re\alpha_2\alpha_3 + 0.16666666667 M^2\alpha_3 - 0.00119476191 Re\alpha_1\beta_0(-0.5000000000 Re\alpha_2\alpha_3 + 0.5000000000 M^2\alpha_3) - 0.00019841269 Re\alpha_3^2)\beta_1 - 0.000198412684\beta_0 Re\alpha_3^2)\ z^7 + (-0.00002755731923 M^2 Re\alpha_3^2 + 0.00001377865962 Re\alpha_1\alpha_3^2\beta_0 - 0.00005511463848 Re\alpha_3\beta_0(-0.5000000000 Re$$

$\alpha_2\alpha_3 + 0.5000000000M^2\alpha_3) - 0.0003306878309Re\beta_0(-0.008333333334Re\alpha_1\alpha_3 + 0.0083$
$33333334M^2\alpha_3)\alpha_3)\beta_1 z^9 + (9.018759018\ 0^{-7}Re^2\alpha_3^2\beta_0 - 0.001262626263Re\beta_0^2(-0.008333$
$33334Re\alpha_1\alpha_3 + 0.08333333334M^2\alpha_3)(-0.5000000000Re\alpha_2\alpha_2\alpha_3 + 0.5000000000M^2\alpha_3))$
$\beta_1 z^{11} + (0.000002428127428Re^2\beta_0^2(-0.008333333334Re\alpha_2\alpha_3 + 0.008333333334M^2\alpha_3)$
$\alpha_3^2 + 1.156251156\ 10^{-8}Re^2\alpha_3^2\beta_0^2(-0.5000000000Re\alpha_2\alpha_3 + 0.500000000M^2\alpha_3)\beta_0 z^{13} -$
$2.5235640311\ 10^{-10}Re^3\beta_0^2\alpha_3^4\beta_1 z^{15}$, (41)
⋮

Now, superseding the second approximate in Eq. (10) to extract the residual $\tilde{R}$, which becomes

$$\tilde{R}(z,\beta_0,\beta_1) = D\left(\frac{d^4A_m(z)}{dz^4}, \frac{d^3A_m(z)}{dz^3}, \frac{d^2A_m(z)}{dz^2}, A_m\right),$$
$$= \frac{d^4A_2(z)}{dz^4} - M^2\frac{d^2A_2(z)}{dz^2} + ReA_2(z)\frac{d^3A_m(z)}{dz^3}, \quad (42)$$

by using Eq. (11) and Eq. (12) to find the values of β_0 and β_1 as follow:

$$\tilde{J}(\beta_0,\beta_1) = \int_0^1 \tilde{R}^2(z,\beta_0,\beta_1)\,dz\,, \quad (43)$$

For example, when take parameters $Re = 1$, $M = 1$, Y=1 the values of the constant are

$\beta_0 = 0.8741438062$ $\beta_1 = 0.8754891051,$ $\alpha_1 = 1.523846385,$ and $\alpha_3 = -3.210078888.$

5. The Analysis of the Convergence

The convergence of the approximate analytical solutions resulting from applying OPTM to solve the non-linear equations is studied with the aid of the convergence theorem and the convergence condition. Firstly, these solutions obtained by OPTM can be viewed in a different way as follows:

A_0=φ_0 , $(A_c)_m = \varphi_{m+1}$, (44)

Sequentially, other solutions can be determined in the following iterations:

$$A_0 = \varphi_0\,,$$
$$A_1 = A_0 + \beta_0(A_c)_0 = \varphi_0 + \varphi_1\,,$$
$$A_2 = A_1 + \beta_1(A_c)_1 = \varphi_0 + \varphi_1 + \varphi_2, \quad (45)$$
$$\vdots$$
$$A_{m+1} = A_m + \beta_m(A_c)_m = \varphi_0 + \varphi_1 + \varphi_2 + \cdots + \varphi_{m+1} = \sum_{i=0}^{m+1}\varphi_i\,.$$

Consequently, the values of $\beta_m\ is$ substituted in Eq. (45) to obtain $A_{m+1}(z)$. The approximate analytical solution required in the form of the power series can be represented as:

$A(z)$=$lim_{m\to\infty}\ A_{m+1}$=$\sum_{i=0}^{\infty}\beta_i$. (46)

Theorem 5.1: Let F be a Banach space denoted with a suitable norm $\|.\|$ over which the series $\sum_{i=0}^{m}\varphi_i$ is defind with assume that initial guess A_0= φ_0 remains inside the ball of the solution $A(z)$. The series solution $\sum_{i=0}^{\infty}\varphi_i$ converges if there is a S such that $\|\varphi_{m+1}\| \le S\|\varphi_m\|$.

Proof: To prove the given theorem, we must prove $\{A_m\}_{i=0}^{\infty}$ is a Cauchy sequence in F it depending on the sequence of solutions in the Eq. (45). In order to fulfil this condition, we take into consideration the following

$$\|A_{m+1} - A_m\| = \|\varphi_{m+1}\| \leq S\|\varphi_m\| \leq S^2\|\varphi_{m-1}\| \leq \cdots \leq S^{m+1}\|\varphi_0\|,$$

For every $m, k \in N, m \geq k$, obtain

$$\begin{aligned}\|A_m - A_k\| &= \|(A_m - A_{m-1}) + (A_{m-1} - A_{m-2}) + \cdots + (A_{k+1} - A_k)\|,\\ &\leq \|A_m - A_{m-1}\| + \|A_{m-1} - A_{m-2}\| + \cdots + \|A_{k+1} - A_k\|,\\ &\leq S^m\|\varphi_0\| + S^{m-1}\|\varphi_0\| + \cdots + S^{k-1}\|\varphi_0\|\\ &= \frac{1 - S^{m-k}}{1 - S} S^{k+1}\|\varphi_0\|.\end{aligned}$$

Since it is common knowledge $0 < S < 1$, One can get results from Eq. (46)

$$\lim_{m,k\to\infty} \|A_m - A_k\| = 0.$$

Finally, $\{A\}_{m=0}^{\infty}$ is a Cauchy sequence in F and this means that the solution of the series (45) is convergent. The proof is complete.

From Theorem 5.1, we can derive the necessary condition for convergence of the solutions obtained by the method as follows:

Definition 5.2: Let φ be the solution extracted from OPIM. The basic condition for convergence can be represented in the following form

$$£^i = \frac{\|\varphi_{m+1}\|}{\|\varphi_m\|}, \qquad i = 1,2,3, \ldots.$$

If $0 < £, £^1, £^2, \ldots < 1$ can be said that the series $\sum_{i=0}^{\infty} \varphi$ is converges to $A(z)$. The definition of condition convergence is implemented to test convergence. The values of £ (PIM) can be summarized in Table 1 to Table 4 while the values of £ (OPIM) recorded in Table 5 to Table 8 for first-grade magnetohydrodynamics squeezing fluid flow with slip boundary condition. From these tables can be seen that £ is between zero and one, meaning the resulting approximate solutions are converged from both methods.

Table 1
The value of $£^i$ for $Re = 21, M = 10, Y = 0.7,\ \alpha_2 = 0.9319414460, \alpha_3 = 0.04537104490$

	$\|.\|_1$	$\|.\|_2$	$\|.\|_\infty$
$£^1$	0.02905150632	0.02905150632	0.02905150632
$£^2$	0.00807902604	0.00708104107	0.00161580520
$£^3$	0.00005633023	0.00001831562	0.00003237017
⋮	⋮	⋮	⋮

Table 2
The value of $\pounds^i$ for $Re = 1.5, M = 1, Y = 0.8,\ \alpha_2 = 0.6342185038, \alpha_3 = 2.197705146$

	$\|.\|_1$	$\|.\|_2$	$\|.\|_\infty$
$\pounds^1$	0.06691496020	0.06691496020	0.06691496020
$\pounds^2$	0.00945767811	0.00472883905	0.00305720248
$\pounds^3$	0.00040583207	0.00023910611	0.00009483210
⋮	⋮	⋮	⋮

Table 3
The value of $\pounds^i$ for $Re = 4.5, M = 3, Y = 0.6, \alpha_2 = 0.6491103561, \alpha_3 = 1.632123077$

	$\|.\|_1$	$\|.\|_2$	$\|.\|_\infty$
$\pounds^1$	0.01974775649	0.01974775649	0.01974775649
$\pounds^2$	0.00624684273	0.00312342136	0.00163374267
$\pounds^3$	0.00003375265	0.00002663601	0.00000138312
⋮	⋮	⋮	⋮

Table 4
The value of $\pounds^i$ for $Re = 2, M = 1, Y = 0.5,\ \alpha_2 = 0.03176712451, \alpha_3 = 5.624017006$

	$\|.\|_1$	$\|.\|_2$	$\|.\|_\infty$
$\pounds^1$	0.01419964565	0.01419964565	0.01419964565
$\pounds^2$	0.00181637408	0.00090818701	0.00008042671
$\pounds^3$	0.00000743810	0.00000482033	0.00000142679
⋮	⋮	⋮	⋮

Table 5
The value of $\pounds^i$ for $Re = 21, M = 10, Y = 0.7,\ \beta_0 = 1.150455909, \beta_1 = 0.8169371596$

	$\|.\|_1$	$\|.\|_2$	$\|.\|_\infty$
$\pounds^1$	1.121702686	1.121702686	1.121702686
$\pounds^2$	0.212688404	0.142317022	0.1063442021
$\pounds^3$	0.004568261	0.002890644	0.001265190
⋮	⋮	⋮	⋮

Table 6
The value of $\pounds^i$ for $Re = 1.5, M = 1, Y = 0.8,\ \beta_0 = 0.9072339986, \beta_1 = 0.9071861920$

	$\|.\|_1$	$\|.\|_2$	$\|.\|_\infty$
$\pounds^1$	0.07726085585	0.07726085585	0.07726085585
$\pounds^2$	0.00492639704	0.03463198521	0.00252164003
$\pounds^3$	0.00062934210	0.00049355134	0.00021536421
⋮	⋮	⋮	⋮

Table 7
The value of $\pounds^i$ for $Re = 4.5, M = 3, Y = 0.6,\ \beta_0 = 0.7618213763, \beta_1 = 0.9052688660$

	$\|.\|_1$	$\|.\|_2$	$\|.\|_\infty$
$\pounds^1$	0.01610006889	0.01610006889	0.01610006889
$\pounds^2$	0.00457960808	0.00314331342	0.00228980404
$\pounds^3$	0.00009956385	0.00007480125	0.00004003589
⋮	⋮	⋮	⋮

Table 8
The value of $\pounds^i$ for $Re = 2, M = 1, Y = 0.5,\ \beta_0 = 0.8887362278, \beta_1 = 0.8866710640$

	$\|.\|_1$	$\|.\|_2$	$\|.\|_\infty$
$\pounds^1$	0.01250779220	0.01250779220	0.01250779220
$\pounds^2$	0.00135380669	0.00067691533	0.00032785841
$\pounds^3$	0.00005907146	0.00003922049	0.00001032009
⋮	⋮	⋮	⋮

6. Tabular Discussion

Tabular analysis of the effect of a physical parameter such as slip parameter (Y), Hartmman number (M) and Reynolds (Re) on the velocity profile of magnetohydrodynamic squeezing fluid flow between two parallel plates in a porous medium with slip boundary conditions. The convergence of values $\frac{dA(0)}{dz}$ and $\frac{d^3A(0)}{dz^3}$ are explained in Table 9 to Table 13 and can see that the values are fixed for the third order. From Table 14 to Table 17 can be observed that the computed error by L_1-norm, L_2-norm, and L_∞-norm. These tables showed that the error obtained from OPIA is more accurate than the error of PIA. The comparison of the solutions of the differential transformation method, optimal homotopy analysis method, OPIA, and BVP4C are indicated in Table 18 [10]. From this table can be said that the results of OPIA converged to the numerical solution of BVP4C. The current solutions for PIA, OPIA, and BVP4C that appear in Table 19 to Table 21 are close to the numerical solutions. The current solutions for PIA, OPIA BVP4c that appear in Table 19 to Table 21 are close to the numerical solutions.

Table 9
The convergence of the values α_1, α_3 for $Re = 1\ , M = 1\ , Y = 0.01$

Approximation order	α_1	α_3
First order	1.525118943	-3.229696700
Second order	1.523678671	-3.208608669
Third order	1.528346385	-3.210078888
Fourth order	1.528346385	-3.210078888
Fifth order	1.528346385	-3.210078888

Table 10
The convergence of the values α_1, α_3 for $Re = 0.9\ , M = 0.2\ , Y = 0.02$

Approximation order	α_1	α_3
First order	1.565687692	-3.628406435
Second order	1.559603616	-3.566942528
Third order	1.560311541	-3.573358287
Fourth order	1.560311541	-3.573358287
Fifth order	1.560311541	-3.573358287

Table 11
The convergence of the values α_1, α_3 for $Re = 0.8\ , M = 0.4\ , Y = 0.05$

Approximation order	α_1	α_3
First order	1.613116582	-3.883867683
Second order	1.609606516	-3.844640960
Third order	1.609934506	-3.847987778
Fourth order	1.609934506	-3.847987778
Fifth order	1.609934506	-3.847987778

Table 12
The convergence of the values α_1, α_3 for $Re = 0.9\,, M = 0.2\,, Y = 0.01$

Approximation order	α_1	α_3
First order	1.549420157	-3.521738276
Second order	1.543212343	-3.460544103
Third order	1.543945314	-3.467017436
Fourth order	1.543945314	-3.467017436
Fifth order	1.543945314	-3.467017436

Table 13
The convergence of the values α_1, α_3 for $Re = 1.5\,, M = 0.3\,, Y = 0.02$

Approximation order	α_1	α_3
First order	1.429871557	-1.915960307
Second order	1.419633269	-1.835144308
Third order	1.419760999	-1.831638289
Fourth order	1.419760999	-1.831638289
Fifth order	1.419760999	-1.831638289

Table 14
Comparison of computed error of $A(z)$ between PIA and OPIA for $Re = 1, M = 1, Y = 0.01$

Error	PIA	OPIA
L_1	$6.6181317 \times 10^{-10}$	5.41644×10^{-10}
L_2	0.0000248	0.0000233
L_∞	0.000069	0.0000495324

Table 15
Comparison of computed error of $A(z)$ between PIA and OPIA for $Re = 0.9, M = 0.2, Y = 0.02$

Error	PIA	OPIA
L_1	$1.041580163\times 10^{-8}$	$1.449265700 \times 10^{-9}$
L_2	0.0001020578347	0.00003806924612
L_∞	0.000285260	0.0000679459

Table 16
Comparison of computed error of $A(z)$ between PIA and OPIA for $Re = 0.8, M = 0.4, Y = 0.05$

Error	PIA	OPIA
L_1	$4.984347087 \times 10^{-9}$	$8.593095684 \times 10^{-10}$
L_2	0.00007059990855	0.00002931398247
L_∞	0.0001971298	0.0000517828

Table 17
Comparison of computed error of $A(z)$ between PIA and OPIA for $Re = 0.9, M = 0.2, Y = 0.01$

Error	PIA	OPIA
L_1	$9.358293928\times 10^{-9}$	$1.330580272\times 10^{-10}$
L_2	0.00009673827540	0.0003647711984
L_∞	0.0002704401	0.0000650920

Table 18
Comparison between OPIA, DIM, OHAM, and BVp4c for $A(z)$

Z	OPIA	DIM [10]	OHAM [10]	BVP4c
0.0	0.000000	0.000000	0.000000	0.000000
0.1	0.077993	0.075739	0.075739	0.077993
0.2	0.176009	0.152935	0.152935	0.176009
0.3	0.264103	0.233046	0.233046	0.264103
0.4	0.352423	0.317540	0.317540	0.352423
0.5	0.441350	0.407893	0.407893	0.441350
0.6	0.531781	0.505591	0.505591	0.531781
0.7	0.625672	0.612134	0.612134	0.625672
0.8	0.797006	0.729034	0.729034	0.797006
0.9	0.893402	0.875813	0.875813	0.893402
1.0	1.000000	1.000000	1.000000	1.000000

Table 19
Comparison between PIA and OPIA for $Re = 1, M = 1, Y = 0.01$

z	PIA	BVP4c	OPIA
0.00	0.0000000000	0.0000000000	0.0000000000
0.10	0.1518332387	0.1518482588	0.1518492465
0.20	0.3004620288	0.3004907271	0.3004949625
0.30	0.4426918877	0.4427378936	0.4428977211
0.40	0.5753844867	0.5754312410	0.5754827289
0.50	0.6954063055	0.6954549842	0.6954617248
0.60	0.7996990284	0.7997436881	0.7997898816
0.70	0.8852502669	0.8852849587	0.8853058586
0.80	0.9490463636	0.9491167417	0.9491793503
0.90	0.9883129961	0.9883190359	0.9883227693
1.00	0.9999999994	1.0000000000	1.0000169310

Table 20
Comparison between PIA and OPIA for $Re = 0.9, M = 0.2, Y = 0.02$

z	PIA	BVP4c	OPIA
0.00	0.0000000000	0.0000000000	0.0000000000
0.10	0.1553662759	0.1554297968	0.1554662701
0.20	0.3071769040	0.3072988807	0.3072775139
0.30	0.4519269766	0.4520942380	0.4521857492
0.40	0.5861989863	0.5863952290	0.5864944640
0.50	0.7067093171	0.7069125713	0.7069967996
0.60	0.8103346810	0.8105196107	0.8105438011
0.70	0.8943331910	0.8942746775	0.8944060485
0.80	0.9553545691	0.9559341767	0.9559696330
0.90	0.9914375689	0.9914568227	0.9914843469
1.00	0.9999999999	1.0000000000	1.000209706

Table 21
Comparison between PIA and OPIA for $Re = 0.9, M = 0.2, Y = 0.01$

z	PIA	BVP4c	OPIA
0.00	0.0000000000	0.0000000000	0.0000000000
0.10	0.1538170845	0.1538105612	0.1538170790
0.20	0.3041787738	0.3041662766	0.3041786059
0.30	0.4476754689	0.4476580252	0.4476743777
0.40	0.5809862457	0.5809656802	0.5809822442
0.50	0.7009161282	0.7008949591	0.7009061999
0.60	0.8044255048	0.8044083188	0.8044175122
0.70	0.8886500525	0.8886463488	0.8886676219
0.80	0.9509102999	0.9509407326	0.9509818305
0.90	0.9887107773	0.9888187384	0.9897635606
1.00	0.9999729598	1.0000000000	0.9999995837

7. Graph Discussion

Figure 2(a) and Figure 2(b) display the impact of increasing M and Re with fixed Y. These figures lead to a decrease in the velocity. Figure 2(c) explains the effect of Y on the velocity profile $A(z)$ which though this figure displays the increment of the velocity profile. Figure 3(a) illustrates the impact of the non-slip boundary when the Reynolds number and Hartmann number are equal. This figure shows a decrease in the velocity of the fluid. The consequences of decreasing the slip parameter Y and increasing the Reynolds number and Hartmann number with M > Re and M < Re are shown in Figure 3(b) and Figure 3(c). These resulted in a reduction in velocity.

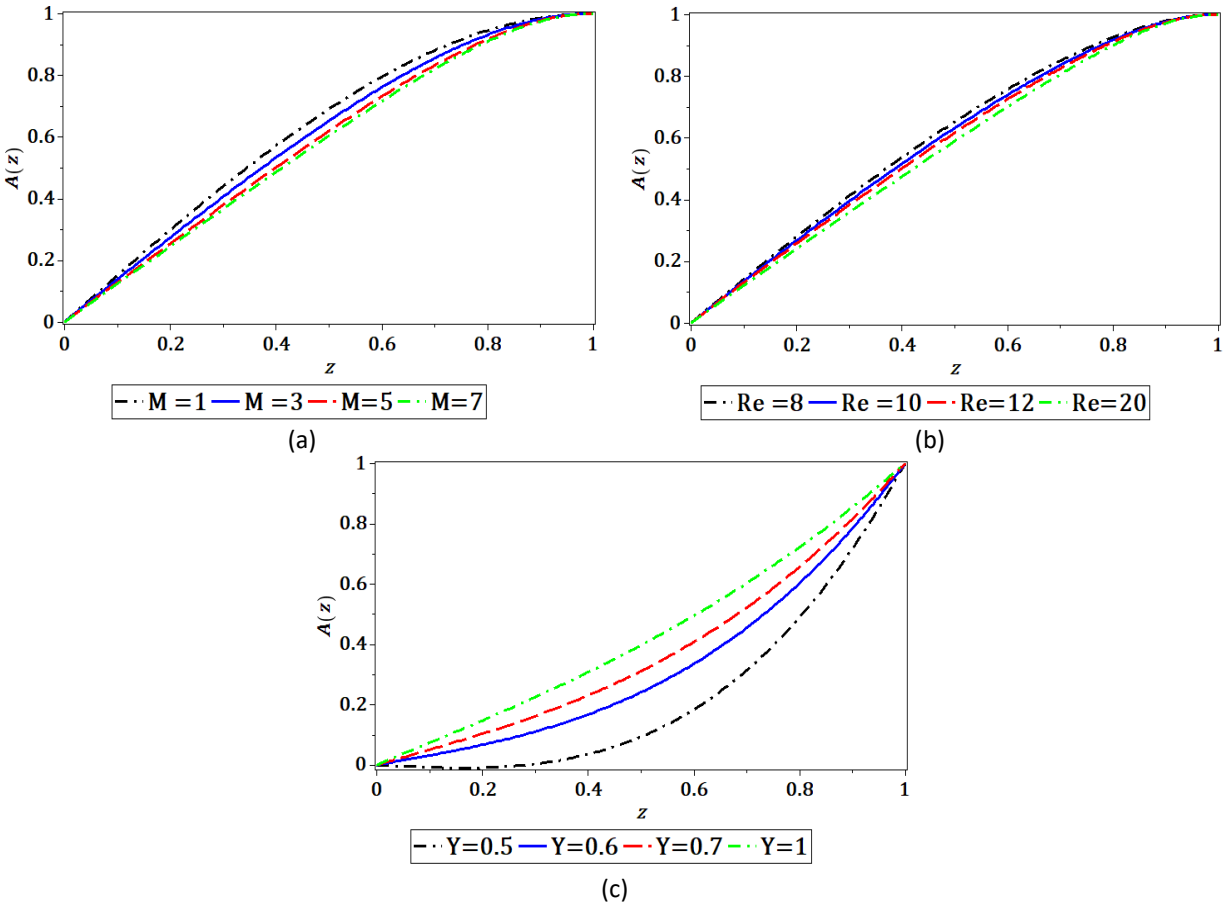

Fig. 2. The curves of the A(z) for different values of (a) Re=1, Y=0; (b) M=1, Y=0; (c) Re=1, M=0

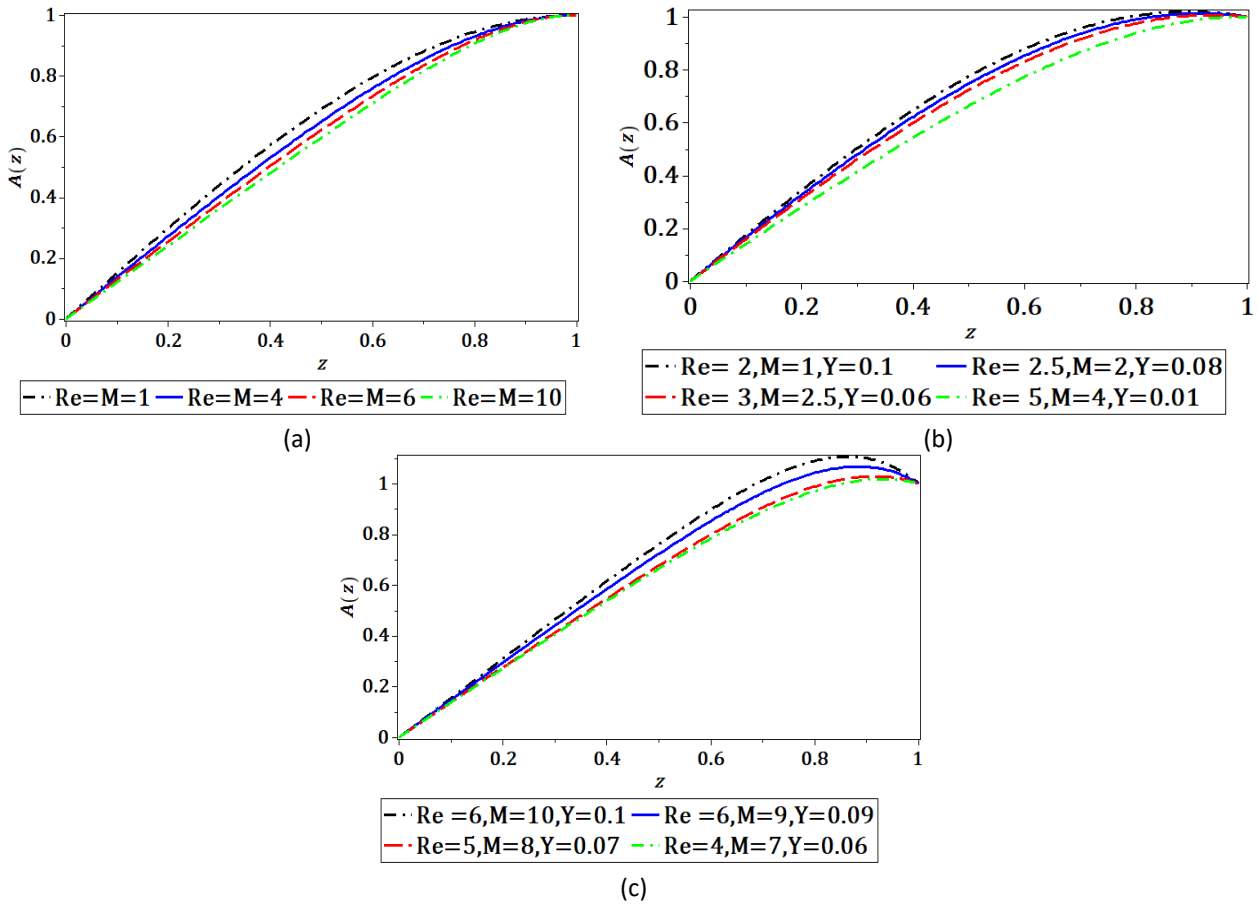

Fig. 3. The curves of the A(z) for different values when (a) Re=M and Y=0; (b) slip parameter when $M < Re$; (c) slip parameter when $M > Re$

Figure 4 displayed the behavior of the streamlines for various Hartmann numbers with the fixed slip parameter and Reynolds number. Figure 5 indicates the effect of the change in Reynolds number with the fixed slip parameter and Hartmann number. From these figures can be determined that the form of the flow function is curves that do not intersect. It can be seen from this table that the behavior of the curves is similar when the values of the physical parameters are small.

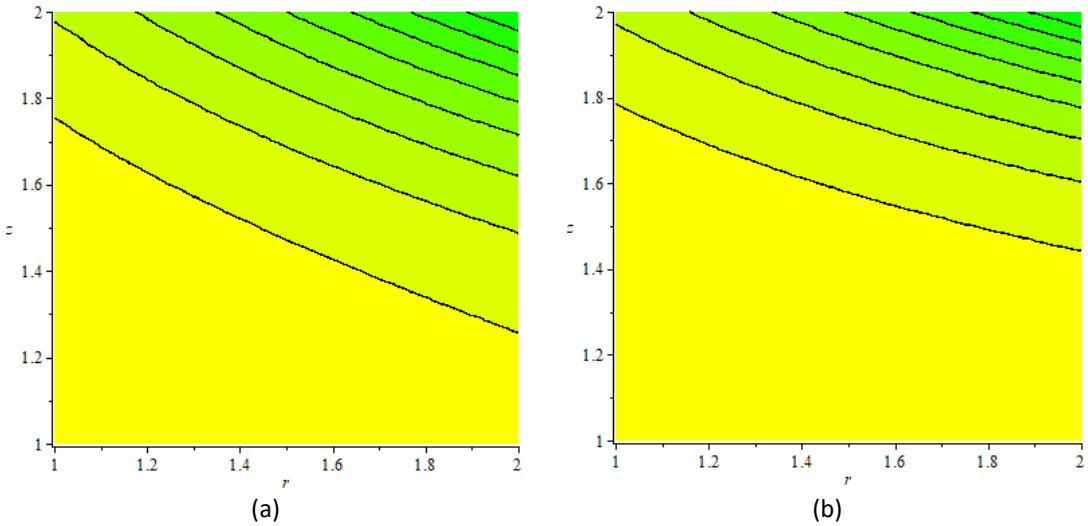

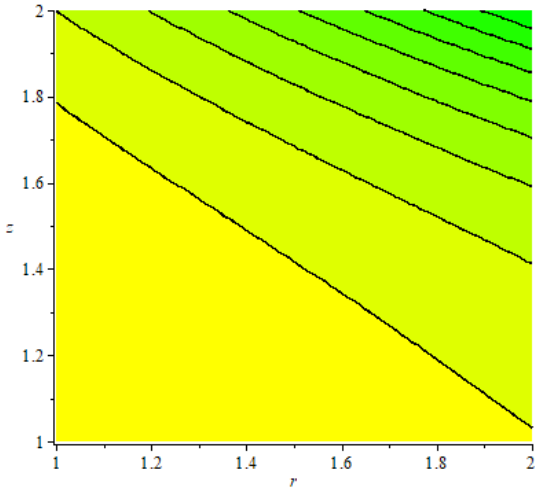

(c)

Fig. 4. The manner of the streamlines, (a) $= 10, Re = 4, Y = 1$; (b) $M = 20, Re = 4, Y = 1$; (c) $M = 30, Re = 4, Y = 1$

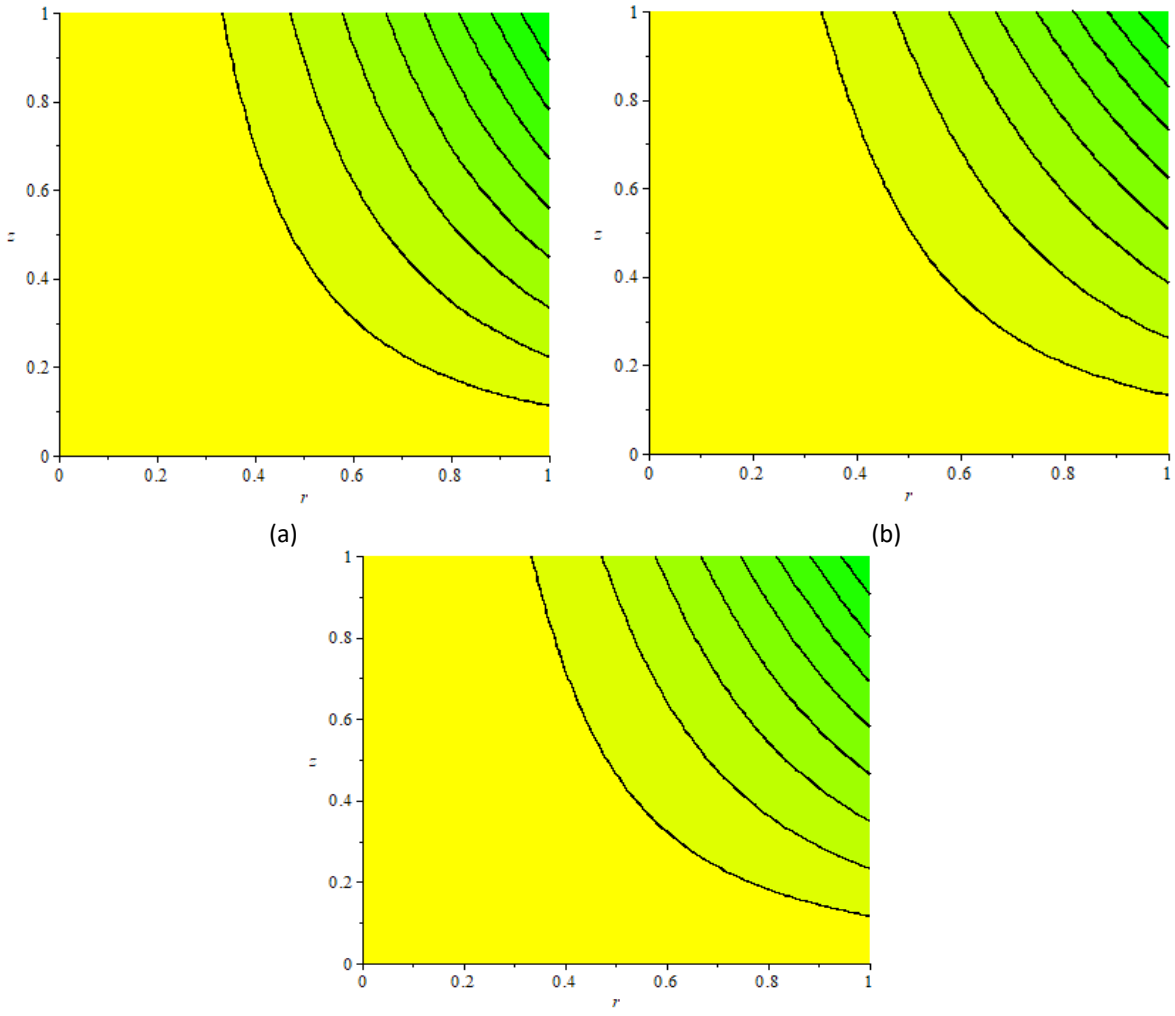

(a) (b)

(c)

Fig. 5. The manner of the streamlines, (a) $= 3, Re = 4, Y = 0.8$; (b) $M = 3, Re = 10, Y = 0.8$; (c) $M = 3, Re = 15, Y = 0.8$

From Figure 6 the behaviour of the curvatures of the streamline far from the z-axis and r-axis can be seen. In Figure 7 the streamline is extended in the direction of the z-axis and the r-axis when the Hartmann number increases. In fluid mechanics, a flow function can determine the path of imaginary particles suspended and carried along with a fluid. In continuous flow, the streamlines are stationary but the fluid is moving. Physically, the fluid velocity is relatively high, and the flow is combined. While they are opened when the fluid is relatively still.

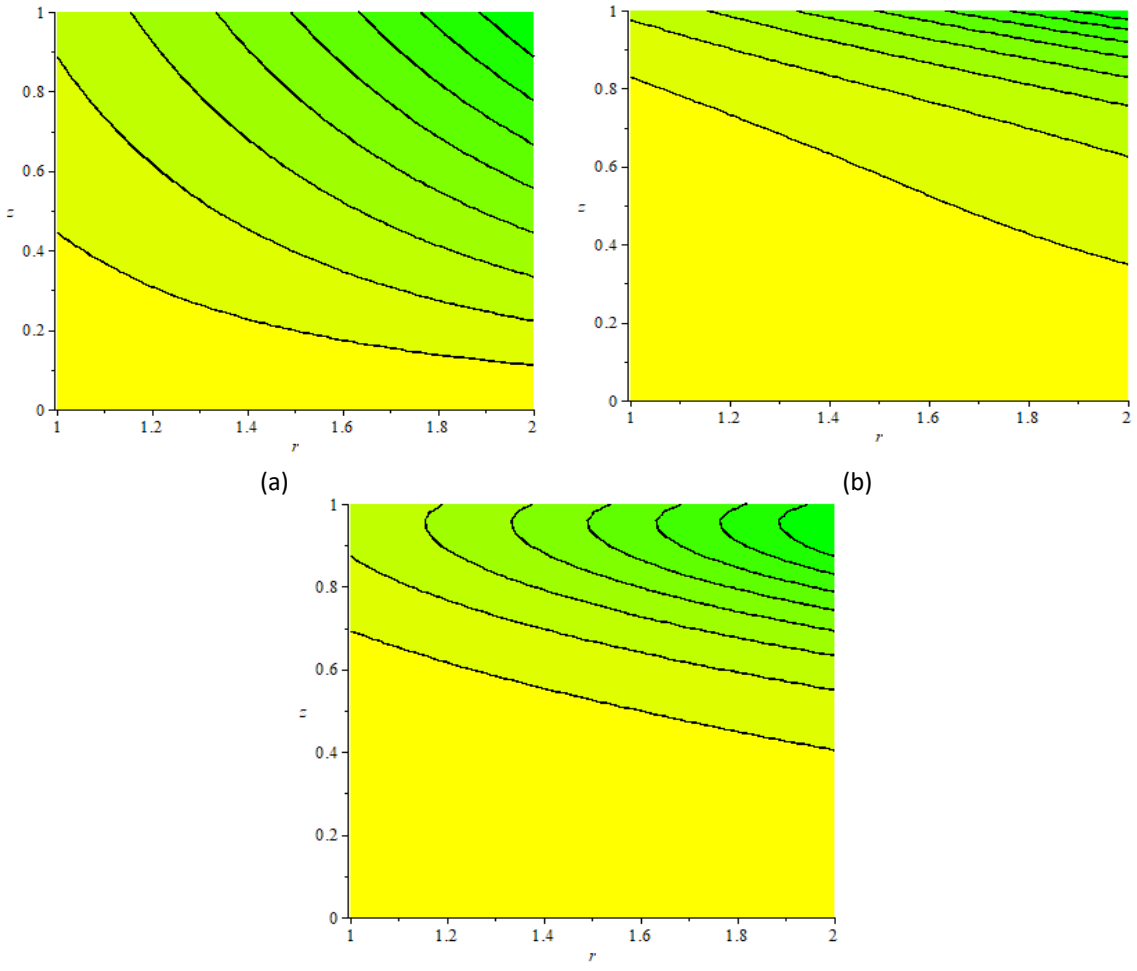

Fig. 6. The manner of the streamlines, (a) $= 10, Re = 50, Y = 0.5$; (b) $M = 10, Re = 400, Y = 0.3$; (c) $M = 10, Re = 1000, Y = 0.8$

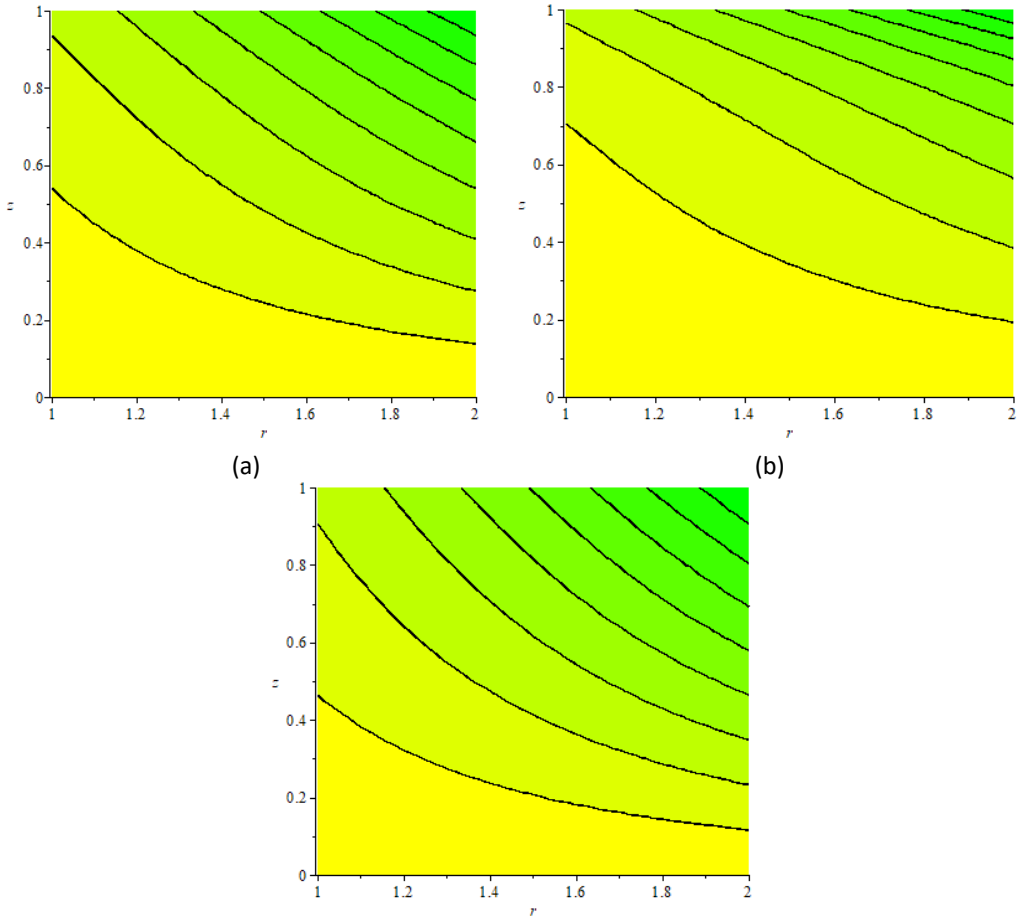

Fig. 7. The manner of the streamlines, (a) $= 10, Re = 20, Y = 0.6$; (b) $M = 40, Re = 20, Y = 0.2$; (c) $M = 100, Re = 20, Y = 0.7$

Physically, an increase in the magnetic parameter causes the Lorentz force to be promoted along the vertical direction, increasing resistance to fluid flow motion and lowering the velocity distribution. In this instance, the magnetic field is the parameter of flow applied perpendicularly to produce force. The magnetic field is utilized to control the fluid's movement because this force has the potential to decrease it. The velocity field is affected by the Reynolds number traveling from close to the cylinder too far away resulting in a discernible reduction in velocity. Eventually, it disappears completely from the surface. The high Reynolds number, which lowers friction between the liquid and the surface, is the cause of this disappearance.

8. Conclusions

In this study, the perturbation iteration algorithm and optimal perturbation iteration algorithm to find the Approximate of the first-grade MHD squeezing fluid flow with boundary conditions are discussed. These approaches have been used to determine the series solution of the velocity profile. The effect of all physical parameters on the behavior of approximate analytical solutions was also studied, which has many applications. One of the applications is the polymer process. Polymers play a key role in everyday use because of their unique properties. However, adding polymers to the water will change the friction coefficient of the pipes in the case of turbulent flow. They are also practical means of reducing hydraulic resistance or friction losses, which have been important for a long time in light of developments in the fields of industry, agriculture, transport of oil and its derivatives, and

the widespread use of water for irrigation. Agriculture and power plants. Especially thermal plants have become less resistant. The most important scientific and technological topics are hydraulic components and increased fluid flow velocity. Conclusions deduced from the current results that are extracted from solving this problem are as follows:

i. The perturbation iteration algorithm and optimal perturbation iteration algorithm are efficient and successful approaches for solving the first-grade MHD squeezing fluid flow with boundary conditions.
ii. The optimal perturbation iteration algorithm results demonstrate a high degree of agreement with the numerical values by BVP4C.
iii. The numerical solution obtained by BVP4C is used to validate the varying order of the approximate solution obtained using the perturbation Iteration Algorithm and optimal perturbation iteration algorithm. This work shows full compatibility when comparing with perturbation iteration algorithm and optimal perturbation iteration algorithm by looking at the results obtained in the tables and figures when controlling the values of physical parameters. As well as it can be said that these approaches are important for work to solve the turbulent flow problem. The presented tables show good agreement and excellent flow results in both divergent and convergent channels, that is good viscosity and a certain density show good flow. The future study of this method is done by expanding the horizons of working on nanofluid by taking fluid with higher densities. Expanding the application of the PIA to winder classes of fluid problems such as the five-dimensional. Application of PIA for solving fractional fluid flow problems.

Acknowledgment
This research was not funded by any grant.

References

[1] Papanastasiou, Tasos, Georgios Georgiou, and Andreas N. Alexandrou. *Viscous fluid flow*. CRC Press, 1994.
[2] Grimm, R. J. "Squeezing flows of Newtonian liquid films an analysis including fluid inertia." *Applied Scientific Research* 32 (1976): 149-166. https://doi.org/10.1007/BF00383711
[3] Ghori, Q. K., M. Ahmed, and A. M. Siddiqui. "Application of homotopy perturbation method to squeezing flow of a Newtonian fluid." *International Journal of Nonlinear Sciences and Numerical Simulation* 8, no. 2 (2007): 179-184. https://doi.org/10.1515/IJNSNS.2007.8.2.179
[4] Rhoades, Lawrence J., Ralph L. Resnick, Ted O'Bradovich, and Steven C. Stegman. *Abrasive flow machining of cylinder heads and its positive effects on performance and cost characteristics*. No. 962502. SAE Technical Paper, 1996. https://doi.org/10.4271/962502
[5] Le Roux, Christiaan. "Existence and uniqueness of the flow of second-grade fluids with slip boundary conditions." *Archive for Rational Mechanics and Analysis* 148 (1999): 309-356. https://doi.org/10.1007/s002050050164
[6] Ran, X. J., Q. Y. Zhu, and Y. Li. "An explicit series solution of the squeezing flow between two infinite plates by means of the homotopy analysis method." *Communications in Nonlinear Science and Numerical Simulation* 14, no. 1 (2009): 119-132. https://doi.org/10.1016/j.cnsns.2007.07.012
[7] Hayat, T., and S. Abelman. "A numerical study of the influence of slip boundary condition on rotating flow." *International Journal of Computational Fluid Dynamics* 21, no. 1 (2007): 21-27. https://doi.org/10.1080/10618560701347003
[8] Ebaid, A. "Effects of magnetic field and wall slip conditions on the peristaltic transport of a Newtonian fluid in an asymmetric channel." *Physics Letters A* 372, no. 24 (2008): 4493-4499. https://doi.org/10.1016/j.physleta.2008.04.031
[9] Abelman, S., E. Momoniat, and T. Hayat. "Steady MHD flow of a third grade fluid in a rotating frame and porous space." *Nonlinear Analysis: Real World Applications* 10, no. 6 (2009): 3322-3328. https://doi.org/10.1016/j.nonrwa.2008.10.067

[10] Ullah, Inayat, Hamid Khan, and M. T. Rahim. "Approximation of first grade MHD squeezing fluid flow with slip boundary condition using DTM and OHAM." *Mathematical Problems in Engineering* 2013, no. 1 (2013): 816262. https://doi.org/10.1155/2013/816262
[11] Hayat, T., A. Shafiq, A. Alsaedi, and S. A. Shahzad. "Unsteady MHD flow over exponentially stretching sheet with slip conditions." *Applied Mathematics and Mechanics* 37 (2016): 193-208. https://doi.org/10.1007/s10483-016-2024-8
[12] Shafiq, Anum, Sumaira Jabeen, T. Hayat, and A. Alsaedi. "Cattaneo–Christov heat flux model for squeezed flow of third grade fluid." *Surface Review and Letters* 24, no. 07 (2017): 1750098. https://doi.org/10.1142/S0218625X17500986
[13] Naseem, Anum, Anum Shafiq, Lifeng Zhao, and M. U. Farooq. "Analytical investigation of third grade nanofluidic flow over a riga plate using Cattaneo-Christov model." *Results in Physics* 9 (2018): 961-969. https://doi.org/10.1016/j.rinp.2018.01.013
[14] Akaje, Wasiu, and B. I. Olajuwon. "Impacts of Nonlinear thermal radiation on a stagnation point of an aligned MHD Casson nanofluid flow with Thompson and Troian slip boundary condition." *Journal of Advanced Research in Experimental Fluid Mechanics and Heat Transfer* 6, no. 1 (2021): 1-15.
[15] Lavilles, Francis Dominic H., Wendell Ace Dela Cruz, and Bonifacio T. Doma Jr. "CFD Analysis of the Choledynamic Flow Characteristics of a Patient with Gallbladder Carcinoma." *CFD Letters* 17, no. 5 (2024): 1-11. https://doi.org/10.37934/cfdl.17.5.111
[16] Lajnef, Mariem, Mabrouk Mosbahi, Zied Driss, Emanuele Amato, Tullio Tucciarelli, Marco Sinagra, and Calogero Picone. "Numerical Model Parameters Impact on Savonius Wind Rotor Performance." *CFD Letters* 17, no. 5 (2024): 58-75. https://doi.org/10.37934/cfdl.17.5.5875
[17] Rehman, Muhammad Zia Ur, Roman Kalvin, Muhammad Zain Ul Abideen, Muhammad Waqas Mustafa, and Juntakan Taweekun. "Implementation of EFI System in 70cc Bike." *Semarak Engineering Journal* 6, no. 1 (2024): 1–10. https://doi.org/10.37934/sej.6.1.110
[18] Niknahad, Ali, and Abdolamir Bak Khoshnevis. "Numerical Study and Comparison of Turbulent Parameters of Simple, Triangular, and Circular Vortex Generators Equipped Airfoil Model." *Journal of Advanced Research in Numerical Heat Transfer* 8, no. 1 (2022): 1–18.
[19] Nadeem, Muhammad, Imran Siddique, Fahd Jarad, and Raja Noshad Jamil. "Numerical Study of MHD Third-Grade Fluid Flow through an Inclined Channel with Ohmic Heating under Fuzzy Environment." *Mathematical Problems in Engineering* 2021, no. 1 (2021): 9137479. https://doi.org/10.1155/2021/9137479
[20] Rashid, Farhan Lafta, Hasan Qahtan Hussein, and Asaad Salim Bded. "Numerical simulation of fluid flow and heat transfer in wellbore." *Journal of Advanced Research in Fluid Mechanics and Thermal Sciences* 60, no. 1 (2019): 60-70.
[21] Nadeem, Muhammad, Imran Siddique, Jan Awrejcewicz, and Muhammad Bilal. "Numerical analysis of a second-grade fuzzy hybrid nanofluid flow and heat transfer over a permeable stretching/shrinking sheet." *Scientific Reports* 12, no. 1 (2022): 1631. https://doi.org/10.1038/s41598-022-05393-7
[22] Nadeem, Muhammad, Imran Siddique, Fahd Jarad, and Raja Noshad Jamil. "Numerical Study of MHD Third-Grade Fluid Flow through an Inclined Channel with Ohmic Heating under Fuzzy Environment." *Mathematical Problems in Engineering* 2021, no. 1 (2021): 9137479. https://doi.org/10.1155/2021/9137479
[23] Al-Saif, A. J. A., and Abeer Majeed Jasim. "Analytical investigation of the MHD Jeffery-Hamel flow through convergent and divergent channel by new scheme." *Engineering Letters* 27, no. 3 (2019): 646-657.
[24] Jasim, Abeer M. "Analytical approximation of the first grade MHD squeezing fluid flow with slip boundary condition using a new iterative method." *Heat transfer* 50, no. 1 (2021): 733-753. https://doi.org/10.1002/htj.21901
[25] Hughes, W. F., and R. A. Elco. "Magnetohydrodynamic lubrication flow between parallel rotating disks." *Journal of Fluid Mechanics* 13, no. 1 (1962): 21-32. https://doi.org/10.1017/S0022112062000464